

Notes on mathematical techniques in rotational and non-rotational cylindrical disks

Jacob Nagler
NIRC,
Haifa, Givat Downes
ISRAEL
Jacobyan123@gmail.com

Abstract: - This paper presents new fresh theoretical expressions development for four special cases. The first case concerns steady-state rotating disk made of functionally graded material (FGM) whilst its material properties and geometry are both varying exponentially. In addition, the disk is subjected to thermal loadings, which have also been considered during calculation. Fully generalized analytical expressions for the displacement and the stress-strain relationships dependent on the material and geometrical parameters as well as on the rotational/spinning velocity and temperature conditions (thermal stresses) subjected to mechanical loadings, have been developed analytically using MAPLE program for special case – extending the analytic study performed by Wen-feng Lin. The second case concern three solid bodies' cylinders that are rotating in triangle partially contact configuration, such as there motion is dependent on each other. The main rationalism is to derive analytic expressions for their stability estimation using simple kinematic relations and body-force diagram as dependent on their geometry and the angular velocity. Finally, the third case concern asymmetrical beam/shaft section analysis in the context of moment instability involved with broad connection to increase the stability interval in relative to the center of mass location.

Key-Words: Disk; Cylinder; FGM; Angular velocity; Exponential variable properties; Thermal stress; Stability; Friction; Contact; Asymmetric beam; Connection joint width; Center of mass.

1 Introduction

The case of rotating hollow cylinder made of functionally graded materials (FGM) varying exponentially under thermal and mechanical loadings has been examined mainly numerically and semi-analytically as will elaborated here.

The applications of such product are expressed in special components design and manufacturing, as cylindrical and annular components: mandrel, thick circular plates, special bearings, shafts (rotational beams), discs, brake disks, dampers & isolators, heat insulations and casings in the mechanical and aerospace industries.

Many researchers have studied the numerical approach during the last two decades. Durodola and Attia [1] have developed numerical direct method code to solve FGM rotating hollow disk without the thermal effect and without varying its thickness, only its Young modulus parameter was varied exponentially. One decade later, Damircheli and Azadi [2] have developed finite element (FE) code that was compared to analytic solution for a rotating cylinder with thermal expansion and geometry

varying according to power-law distribution but not exponentially. In 2010, Asfar and Go [3] have developed numerical solution (by finite element method) to the problem of rotating circular disk with thermal effect and under mechanical loadings but with constant geometry.

Thorough review on the power-law distribution of FGM hollow cylinder until 2012 has been presented by Ali et al. [4]. In 2015 thermoelastic analysis of variable thickness based on F.E. method has been performed by Thawait and Sondhi [5]. The material properties has been varied exponentially but geometry was distributed by the power law distribution. However, time-dependent generalized form of the differential equation appear in Zheng et al. [6, 7] even though they solved power-law problem using FEM. About three years later, Allam and Zenkour [8] have investigated numerically the exponential effect vs. the power-law form for two different rotating cylinder geometries while the FGM properties were varied according to power-law and thermal effect was also considered.

In 2019, Thawait *et al.* [9] has performed FEM for elastic exponential rotational FGM cylinder case without thermal effect while the annular disk geometry was based on power-law distribution.

Many researchers including Baghani *et al.* [10] who developed generalized semi-analytical-numerical solution without thermal effect for rotational annular disk have studied the semi-analytical approach. Note that Behravan-Rad and Shariyat [11] have proposed a thorough electromagnetic-analysis on FGM circular plate-disks without rotation and without thermal effect. In addition, Shariyat and Mohammadjani [12, 13] have solved semi-analytically the three-dimensional problem of circular hollow disk made of FGM with constant geometry thickness and without thermal effects. In 2021, Sarkar and Rahman [14] have proposed numerical scheme to solve the fully FGM disk problem with exponential material and geometrical varying properties subjected to thermal and mechanical loadings.

A brief analytical approach review in the context of exponential variable distribution of FGM properties and annular geometry will be introduced.

In 2002 Eraslan and Orcan [15] have developed analytic solution to a rotating solid disk of exponentially varying thickness with constant material properties and without thermal effect.

A different cases of density alongside Young modulus material properties of rotating FGM uniform disk thickness varying exponentially subjected to uniform thermal loading were investigated semi-analytically by Zenkour [16-19]. Some extension was performed for the case of elastic-plastic deformation by Sahni and Sharma [20] whom investigated in 2016 an FGM rotating disk with exponential variable geometry thickness and density without thermal effect was examined analytically by Sahni & Sharma.

In 2006, Chen *et al.* [20] have performed three-dimensional analytic solution to FGM rotating disc without thermal effect and with constant geometry but material properties were varying exponentially. In 2011, thermoelastic analytic solution defined by finite element formulation was derived by Sharma *et al.* [21] for the case of rotating constant circular disk geometry with thermal and FG exponential material properties. In 2015, Jabbari *et al.* [22] have defined the generalized FGM non-linear differential equation considering the rotation, thermal and mechanical loadings for exponential varying properties (geometrical and material) and also compared it to

the power law distribution. However, they solved the exponential case semi-analytically and have not presented the fully explicit solution as dependent on Whittaker's functions or other explicit function representation. Later, this solution have become clearer in further investigations as will be elaborated here.

One year later, Manthena *et al.* [23] have solved three-dimensional hollow elliptic-cylinder FGM obeying the exponential law, subjected to uniform temperature by solving uncoupled stress and temperature equations. Although current problem will involve solving coupled thermal and stress equilibrium. In the same year Dai [24] has developed semi-analytic solution to FGM disk with variable exponential properties with power-law variable thickness including thermal effect. In 2019, analytic exact solution of constant geometry thickness but with varying exponential properties under non-symmetric thermal and mechanical loads was derived by Akbari and Ghanbari [25] based on Whittaker's functions. At the same time, Wen-feng Lin [26] has developed fully analytic solution based on Whittaker's functions for the case of variable exponential thickness with exponential properties and under thermal and mechanical loads. Recent studies performed by Lin have examined particular cases of the generalized analytic solution including states with and without thermal effect [27 - 29]. Similar semi-analytic study without rotation and without thermal effect was performed by Paul and Sahni [30]. However, Lin [26-29] has not developed an important particular case, which will be developed analytically in the current essay and might represent important cases of rotating FGM cylinders or disks subjected to either mechanical and thermal loads with exponential geometry and material properties that fulfill an interested physical quality that the exponential power of the geometry equals to the exponential power of the Young modulus of elasticity magnitude. Analytically, we will show that the generalized non-linear differential equation has explicit solution and the dependency on the generalized Whittaker's functions is vanished and instead become dependent on simple polynomial form.

The second discussed topic concerning three cylinders that arranged in triangle configuration with partially contact between the upper cylinder and the two other below parallel cylinders. The contact rolling problem of cylinders has been discussed in many fundamentals text books [31]-[33] and advanced studies [34-37]. Koczan and Ziomek [34] have discussed and developed similar

stability problem that concern with balls stability and known as 'Cobblestone model'. Ndiaye *et al.* [35] have investigated the rolling friction effect (dry and wet states for cohesion examination purposes) during particles contact by developing 2D numerical simulations. A generalized control balancing system was developed by Ott and Hyon [36] for generalized oscillating system.

However, here, the second Newton's law kinematics (inertia angular momentum, acceleration – force momentum) of the rotational system with friction will be developed will be developed and discussed in the context of system stability. The relationships between the three cylinders will be based on forced movement of one cylinder that is in contact with the upper cylinder which is in contact with lower cylinder while the contact is based on rotational friction. This system might represent variety of mechanical engineering systems, like open yarn spinning [37], cylindrical painting systems, thread rolling, gears, conveyors, etc.

The third and last topic will concern an asymmetrical beam that expressed in different mass distribution alongside different linear - saw section parts along the longitudinal axis while an expression of an improved broad connection joint that assisting to cope with the mass balance stability will be determined.

To sum it up, the motivation to investigate those problems from simplicity view is important and enables to compare and examine complex engineering problems and solution from simple view and to have relatively simple initial evaluation.

2 Problem Formulation – Rotating FGM hollow cylindrical disk with exponential variable properties

We consider here a solid body FGM cylinder being rotated through its axi-symmetric axis while its geometry and material properties are varied according to the following relations [26-29]:

$$h(r) = h_0 e^{m_1(r-a)/b} \quad (1)$$

$$E(r) = E_0 e^{m_2(r-a)/b} \quad (2)$$

$$\rho(r) = \rho_0 e^{m_3(r-a)/b} \quad (3)$$

$$\alpha(r) = \alpha_0 e^{m_4(r-a)/b} \quad (4)$$

$$k(r) = k_0 e^{m_5(r-a)/b} \quad (5)$$

while a, b are the inner and outer disk or cylinder radii. $h_0, E_0, \rho_0, \alpha_0, k_0$ are the initial values of the thickness (h), Young's modulus of elasticity (E), the density (ρ), thermal expansion coefficient (α) and thermal conduction coefficient (k), respectively. All the properties can be summarized by the formula:

$$P(r) = P_0 e^{m_i(r-a)/b} \quad (6)$$

where $i = 1, 2, 3, 4, 5$. and P represents the symbols h, E, ρ, α, k .

Assuming plane strain and axis symmetry assumptions where the stress components are not dependent on the tangential direction, we will have the following radial and tangential (circumferential) stress relations dependent the radial direction [26-29]:

$$\sigma_r = \frac{E(r)}{(1+\nu)(1-2\nu)} \left[(1-\nu) \frac{du}{dr} + \nu \frac{u}{r} - (1+\nu) \alpha(r) T(r) \right] \quad (7)$$

$$\sigma_\theta = \frac{E(r)}{(1+\nu)(1-2\nu)} \left[(1-\nu) \frac{u}{r} + \nu \frac{du}{dr} - (1+\nu) \alpha(r) T(r) \right] \quad (8)$$

while u is the displacement function and ν is the Poisson's ratio and $T(r)$ is the temperature function dependent on the radial coordinate (r).

In the case of three dimensional analysis, we will have the perpendicular component in the z - direction will be:

$$\sigma_z = \nu(\sigma_r + \sigma_\theta) \quad (9)$$

The representative general steady-state balance non-linear second order differential equation of motion in polar coordinates is [22, 24, 29]:

$$\frac{1}{r} \frac{\partial}{\partial r} (r h(r) \sigma_r) - \frac{h(r) \sigma_\theta}{r} + \rho(r) h(r) f_r = -\rho(r) h(r) \omega^2 r \tag{10}$$

where f_r is the body force per mass unit term. Next, substituting relations (7) – (8) into Eq. (10) and solving the obtained equation yields the appropriate solution for the displacement formula:

$$u(r) = \left\{ 2bq_1q_4(\omega^2 r^2 + rf_r) + \frac{2b^2q_1q_4}{q_6} [(2r + 1)\omega^2 + f_r] + \frac{4b^3\omega^2q_1q_4}{q_3} \right\} \frac{e^{q_6(\frac{a-r}{b})}}{r} + \frac{q_1q_5q_3}{r} \int r\Delta T(r) e^{m_4(\frac{r-a}{b})} dr + C_1r + \frac{C_2}{r} \tag{10}$$

Where,

$$\begin{aligned} q_1 &= \frac{1 + \nu}{q_3 h_0 E_0 (1 - \nu)}; \\ q_2 &= q_5 - 2\nu + 1; \\ q_3 &= q_6^2; \\ q_4 &= h_0 \rho_0 b (\nu - 1/2) \\ q_5 &= h_0 E_0 \alpha_0 \\ q_6 &= m_1 - m_3 \end{aligned} \tag{11}$$

Whereas the corresponding stress-strain relations (7) – (8) will be obtained by substituting (10) into these expressions as:

$$\sigma_\theta =$$

$$\frac{1}{q_6 q_3^2 (1 + \nu) (-1 + 2\nu)} \left(E_0 e^{-\frac{m_3(-r+a)}{b}} \left(2C_1 \nu q_3 q_6 - e^{-\frac{m_3(-r+a)}{b}} \Delta T(r) \nu q_1 q_3^2 q_4 q_6 r^2 - 2e^{-\frac{m_3(-r+a)}{b}} b f_r q_1 q_3 q_4 q_6 r \right. \right. \\ \left. \left. + 4e^{-\frac{m_3(-r+a)}{b}} b^2 \nu^2 q_1 q_3 q_4 r + 4e^{-\frac{m_3(-r+a)}{b}} b^2 \nu^2 q_1 q_3 q_4 r^2 + 2e^{-\frac{m_3(-r+a)}{b}} f_r \nu q_1 q_3 q_4 q_6^2 r^2 - 2e^{-\frac{m_3(-r+a)}{b}} b \omega^2 q_1 q_3 q_4 q_6^2 \right. \right. \\ \left. \left. + 2e^{-\frac{m_3(-r+a)}{b}} \nu \omega^2 q_1 q_3 q_4 q_6^2 r^3 - 4e^{-\frac{m_3(-r+a)}{b}} b^2 \omega^2 q_1 q_3 q_4 r + \Delta T(r) \alpha_0 e^{-\frac{m_3(-r+a)}{b}} q_6 q_3^2 + 2 \left(\int r \Delta T(r) e^{-\frac{m_3(-r+a)}{b}} dr \right) \nu q_1 q_3^2 q_4 q_6 \right. \right. \\ \left. \left. + C_1 \nu q_3 q_6 r r - 4e^{-\frac{m_3(-r+a)}{b}} b^2 \omega^2 q_1 q_4 q_6 - 2e^{-\frac{m_3(-r+a)}{b}} b^2 \omega^2 q_1 q_3 q_4 - 2e^{-\frac{m_3(-r+a)}{b}} b^2 f_r q_1 q_3 q_4 - C_2 q_6 q_3 - C_1 r r q_6 q_3 - q_1 q_3 q_3^2 \left(\int r \Delta T(r) e^{-\frac{m_3(-r+a)}{b}} dr \right) \right. \right. \\ \left. \left. + 8e^{-\frac{m_3(-r+a)}{b}} b^2 \nu \omega^2 q_1 q_4 q_6 + 4e^{-\frac{m_3(-r+a)}{b}} b^2 \nu \omega^2 q_1 q_3 q_4 + 4e^{-\frac{m_3(-r+a)}{b}} b^2 f_r \nu q_1 q_3 q_4 + \Delta T(r) \alpha_0 e^{-\frac{m_3(-r+a)}{b}} q_6 q_3^2 \nu \right. \right. \\ \left. \left. + 4e^{-\frac{m_3(-r+a)}{b}} b \nu \omega^2 q_1 q_3 q_4 q_6^2 + 2e^{-\frac{m_3(-r+a)}{b}} b \nu \omega^2 q_1 q_3 q_4 q_6 r + 4e^{-\frac{m_3(-r+a)}{b}} b f_r \nu q_1 q_3 q_4 q_6 r \right) \right) \tag{12}$$

$$\sigma_r = -\frac{1}{q_6 q_3^2 (1 + \nu) (-1 + 2\nu)} \left(E_0 e^{-\frac{m_3(-r+a)}{b}} \left(2C_2 \nu q_3 q_6 - 2e^{-\frac{m_3(-r+a)}{b}} \Delta T(r) \nu q_1 q_3^2 q_4 q_6 r^2 \right. \right. \\ \left. \left. - 2e^{-\frac{m_3(-r+a)}{b}} b f_r q_1 q_3 q_4 q_6 r + 4e^{-\frac{m_3(-r+a)}{b}} b^2 \nu \omega^2 q_1 q_3 q_4 r + 4e^{-\frac{m_3(-r+a)}{b}} b^2 \nu \omega^2 q_1 q_3 q_4 r^2 + 2e^{-\frac{m_3(-r+a)}{b}} f_r \nu q_1 q_3 q_4 q_6^2 r^2 \right. \right. \\ \left. \left. - 2e^{-\frac{m_3(-r+a)}{b}} b \omega^2 q_1 q_3 q_4 q_6^2 r^3 + 2e^{-\frac{m_3(-r+a)}{b}} \nu \omega^2 q_1 q_3 q_4 q_6^2 r^2 - \Delta T(r) \alpha_0 e^{-\frac{m_3(-r+a)}{b}} q_6 q_3^2 + 2 \left(\int r \Delta T(r) e^{-\frac{m_3(-r+a)}{b}} dr \right) \nu q_1 q_3^2 q_4 q_6 \right. \right. \\ \left. \left. + C_1 \nu q_3 q_6 r r - 4e^{-\frac{m_3(-r+a)}{b}} b^2 \omega^2 q_1 q_4 q_6 - 2e^{-\frac{m_3(-r+a)}{b}} b^2 \omega^2 q_1 q_3 q_4 - 2e^{-\frac{m_3(-r+a)}{b}} b^2 f_r q_1 q_3 q_4 - C_2 q_6 q_3 - q_1 q_3 q_3^2 \left(\int r \Delta T(r) e^{-\frac{m_3(-r+a)}{b}} dr \right) \right. \right. \\ \left. \left. - 2e^{-\frac{m_3(-r+a)}{b}} \omega^2 q_1 q_3 q_4 q_6^2 r^3 + 8e^{-\frac{m_3(-r+a)}{b}} b^2 \nu \omega^2 q_1 q_3 q_4 q_6 - 4e^{-\frac{m_3(-r+a)}{b}} b^2 \omega^2 q_1 q_3 q_4 r + 4e^{-\frac{m_3(-r+a)}{b}} b^2 \nu \omega^2 q_1 q_3 q_4 \right. \right. \\ \left. \left. - 2e^{-\frac{m_3(-r+a)}{b}} f_r q_1 q_3 q_4 q_6^2 r^2 + q_1 q_3 q_3^2 \Delta T(r) e^{-\frac{m_3(-r+a)}{b}} q_6^2 + 4e^{-\frac{m_3(-r+a)}{b}} b^2 f_r \nu q_1 q_3 q_4 - \Delta T(r) \alpha_0 e^{-\frac{m_3(-r+a)}{b}} q_6 q_3^2 \nu \right. \right. \\ \left. \left. + 4e^{-\frac{m_3(-r+a)}{b}} b \nu \omega^2 q_1 q_3 q_4 q_6^2 + 2e^{-\frac{m_3(-r+a)}{b}} b \nu \omega^2 q_1 q_3 q_4 q_6 r + 4e^{-\frac{m_3(-r+a)}{b}} b f_r \nu q_1 q_3 q_4 q_6 r \right) \right) \tag{13}$$

Assuming that the exponential power of the geometry expression equals to the exponential power of the Young modulus of elasticity magnitude such as $|m_1| \approx |m_2|$ such as $m_1 = -m_2$.

Hence, there is no dependency on the well-known Whittaker function as appear in [26-29] since the opposite power sign cancel each other and allows the polynomial form to be generated. Particular case of (10) could be achieved by using the temperature terms that were obtained by [26-29] or any other obtained function as dependent on the temperature distribution and/or heat rates in the inner/outer surfaces. Additionally, body force coefficient could be assumed to behave as linear, exponential or polynomial radial function.

3 Problem Formulation – Stability of Three rotating cylinders coupled rotation in triangular configuration

Suppose we have three cylinders rotating in triangle configuration as appear in Fig. 1 while the two lower parallel cylinders (B, C) are in contact with the upper cylinder (A) but not with each other. The steady-state coupling rotation mechanism between the three cylinders is based on free rotational whereas only one cylinder rotation movement is forced (C) by engine moment (thrust) T and the motions of the other two cylinders (A and B) are obtained as a result of the motion of the forced cylinder motion. Free body diagram in Cartesian coordinates (X, Y) of each cylinder is presented in Fig. 2. Both lower cylinders are rotating counter-clockwise while the upper cylinder rotation is in the clockwise direction.

Each of the cylinders have constant acceleration velocity ($\alpha_A, \alpha_B, \alpha_C$). Accordingly, each cylinder fulfil in general form that its angular velocity is:

$$\omega_i = \alpha_i t + \omega_{0,i} \quad (14)$$

since $\alpha_i = \frac{\partial \omega_i}{\partial t}$, $\omega_{0,i}$ is the integration - initial rotation velocity value and i subscript symbol represents the cylinders notation A, B, C respectively.

Now, since the velocities of the cylinders edge supply the following equalities:

$$v_A = \omega_A r_A = v_B = \omega_B r_B = v_C = \omega_C r_C, \quad (15)$$

Then by differentiation of Eq. (15) along the time axis, we have the following angular acceleration forms which will be used continually to evaluate the friction coefficients allowing the relative motion between the cylinders:

$$\alpha_B = \frac{\alpha_A r_A}{r_B}, \alpha_C = \frac{\alpha_A r_A}{r_C}, \quad (16)$$

The stability of cylinder A in relative to cylinders B and C motion will be determined and define in accordance with the following physical parameters perspective:

- Geometry: $\delta_{critical}$ critical opening angle which dictates the appropriate height H and distance d (Fig. 1) that enable stability. we would like to define continually the critical opening angle $\delta_{critical}$ ($\delta = 180^\circ - \beta - \gamma$), while the distance and height are dependent on the opening angle.
- Forces: allowance normal forces value.
- Obtained angular velocity: critical value.

Observing the created cantered shaped triangular geometry in Fig. 1, in case the circular centres of cylinders B and C are not collinear, will be treated the same way.

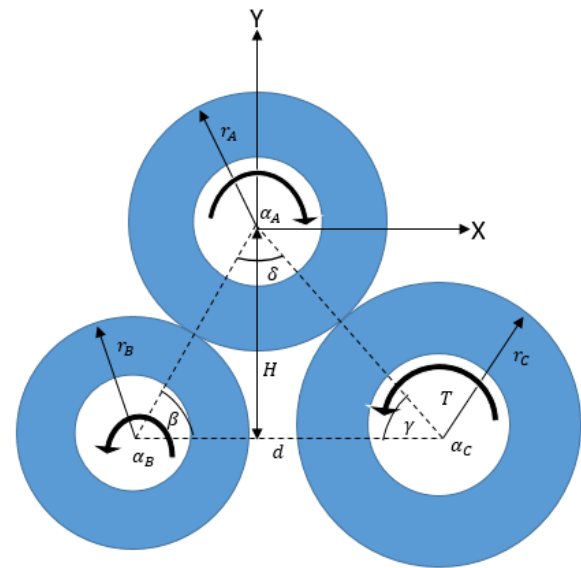


Figure 1: Three rotated cylinders diagram

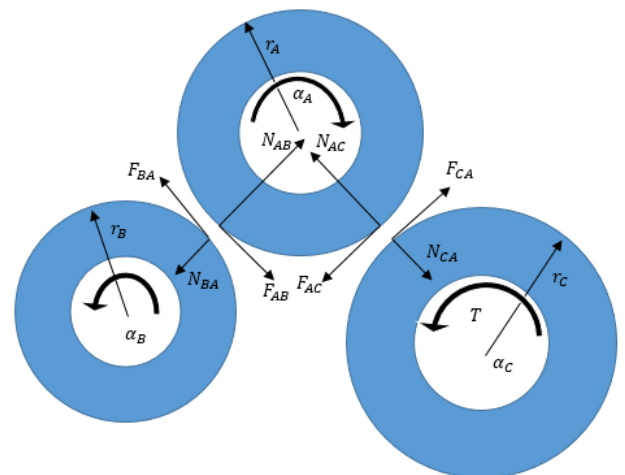


Figure 2: Three rotated cylinders free body force diagram

The equations of motion of the upper cylinder resulting from its own rotation together with the contact based on Newton's second and third laws, respectively, between the two lower cylinders are as following:

$$X: -F_{k,AC} \sin(\gamma) + F_{k,AB} \sin(\beta) - N_{AC} \cos(\gamma) + N_{AB} \cos(\beta) = m_A a_A = m_A \alpha_A r_A \quad (17)$$

Using the geometrical identities $\cos(90 - \delta) = \sin(\delta)$ and similarly $\cos(90 - \beta) = \sin(\beta)$.

$$Y: N_{AC} \sin(\gamma) + N_{AB} \sin(\beta) - F_{k,AC} \cos(\gamma) - F_{k,AB} \cos(\beta) = m_A g \tag{18}$$

whereas $F_{k,AC} = -F_{k,CA}$, $F_{k,BC} = -F_{k,CB}$. Also, the appropriate moments inertia equations of each lower cylinder is:

$$T - F_{k,CA} r_C = \alpha_C I_C \tag{19}$$

$$F_{k,BA} r_B = \alpha_B I_B \tag{20}$$

$$(-F_{k,AC} + F_{k,AB}) r_A = -\alpha_A I_A \tag{21}$$

while the upper cylinder body linear acceleration motion fulfils $a_A = \alpha_A r_A$. Note that the contact between the two lower cylinders ($F_{k,BC} = -F_{k,CB}$, $N_{BC} = -N_{CB}$) is not important here since it has no impact on the upper cylinder stability and in case the two lower cylinders are fixed it even has no effect overall system. Remark that in order to have counter-clockwise motion $F_{k,AB} r_A < F_{k,AC} r_C$ and similarly $T > F_{CA} r_C$.

In addition, the friction roll forces relation with the normal forces will supply:

$$F_{k,CA} = \mu_{CA} N_{CA} \tag{22}$$

$$F_{k,BA} = \mu_{BA} N_{BA} \tag{23}$$

where μ_{CA} , μ_{BA} are the kinetic roll friction coefficients. Accordingly, the normal and friction forces will be evaluated by solving the five algebraic equilibrium expressions (17) – (21) against the five unknowns ($F_{k,AC}$, $F_{k,AB}$, N_{AB} , N_{AC} , α_A) using relations (22)-(23), such as Eq. (17) becomes:

$$F_{1\beta} \alpha_B + F_{1\gamma} \alpha_C + G_{1\gamma} T = r_A \alpha_A \tag{24}$$

$$\text{where, } F_{1\beta} = -\frac{I_B}{r_B m_A} \left[\sin(\beta) + \frac{\cos(\beta)}{\mu_{BA}} \right], \quad F_{1\gamma} = -\frac{I_C}{r_C m_A} \left[\sin(\gamma) + \frac{\cos(\gamma)}{\mu_{CA}} \right] \quad \text{and} \quad G_{1\gamma} = \frac{1}{r_C} \left(\sin(\gamma) + \frac{\cos(\gamma)}{\mu_{CA}} \right).$$

In similar way, Eq. (18) becomes:

$$F_{2\beta} \alpha_B + F_{2\gamma} \alpha_C + G_{2\gamma} T = g \tag{25}$$

$$\text{where, } F_{2\beta} = \frac{I_B}{r_B m_A} \left[\cos(\beta) - \frac{\sin(\beta)}{\mu_{BA}} \right], \quad F_{2\gamma} = \frac{I_C}{r_C m_A} \left[\frac{\sin(\gamma)}{\mu_{CA}} - \cos(\gamma) \right] \quad \text{and} \quad G_{2\gamma} = \frac{1}{r_C} \left(\cos(\gamma) - \frac{\sin(\gamma)}{\mu_{CA}} \right).$$

Note that in case where $\mu_{BA} = tg(\beta)$ or $\mu_{CA} = tg(\gamma)$ the friction forces become zero which is well-known result. In this stage to enable frictional motion, we will require that $\mu_{BA} \geq tg(\beta)$ or $\mu_{CA} \geq tg(\gamma)$.

Also, reformulating (21) using the above relations, yields:

$$J_B \alpha_B + J_C \alpha_C + T J_T = J_A \alpha_A \tag{26}$$

$$\text{whereas } J_A = -\frac{I_A}{r_A}, J_B = -\frac{I_B}{r_B}, J_C = -\frac{I_C}{r_C}, J_T = \frac{1}{r_C}.$$

Solving the linear Eqs. (24) – (26) yields:

$$\alpha_A = \frac{((J_B F_{1\gamma} G_{2\gamma} - J_B F_{2\gamma} G_{1\gamma} - J_C F_{1\beta} G_{2\gamma} + J_C F_{2\beta} G_{1\gamma} + J_T F_{1\beta} F_{2\gamma} - J_T F_{1\gamma} F_{2\beta}) T)}{(J_A F_{1\beta} F_{2\gamma} - J_A F_{1\gamma} F_{2\beta} - J_B r_A F_{2\gamma} + J_C r_A F_{2\beta}) + \frac{(-J_B F_{1\gamma} + J_C F_{1\beta}) g}{J_A F_{1\beta} F_{2\gamma} - J_A F_{1\gamma} F_{2\beta} - J_B r_A F_{2\gamma} + J_C r_A F_{2\beta}}} \tag{27}$$

$$\alpha_B = \frac{(-J_A F_{1\gamma} + J_C r_A) g}{J_A F_{1\beta} F_{2\gamma} - J_A F_{1\gamma} F_{2\beta} - J_B r_A F_{2\gamma} + J_C r_A F_{2\beta}} + \frac{(J_A F_{1\gamma} G_{2\gamma} - J_A F_{2\gamma} G_{1\gamma} - J_C r_A G_{2\gamma} + J_T r_A F_{2\beta}) T}{J_A F_{1\beta} F_{2\gamma} - J_A F_{1\gamma} F_{2\beta} - J_B r_A F_{2\gamma} + J_C r_A F_{2\beta}} \tag{28}$$

$$\alpha_C = -\frac{(-J_A F_{1\beta} + J_B r_A) g}{J_A F_{1\beta} F_{2\gamma} - J_A F_{1\gamma} F_{2\beta} - J_B r_A F_{2\gamma} + J_C r_A F_{2\beta}} - \frac{(J_A F_{1\beta} G_{2\gamma} - J_A F_{2\beta} G_{1\gamma} - J_B r_A G_{2\gamma} + J_T r_A F_{2\beta}) T}{J_A F_{1\beta} F_{2\gamma} - J_A F_{1\gamma} F_{2\beta} - J_B r_A F_{2\gamma} + J_C r_A F_{2\beta}} \tag{29}$$

$$N_{CA} = \frac{\alpha_C I_C}{\mu_{CA} r_C} \tag{30}$$

$$N_{BA} = \frac{\alpha_B I_B}{\mu_{BA} r_B} \tag{31}$$

Now, in order to enable relative dependent frictional motion between the cylinders (A & B, A & C) we will determine the frictional coefficients by assuming (16) to obtain the following linear equations:

$$\frac{(-J_A r_B F_{1\gamma} + J_B r_A F_{1\gamma} + J_C r_A F_{1\beta} - J_C r_A F_{1\beta}) g}{(J_A F_{1\beta} F_{2\gamma} - J_A F_{1\gamma} F_{2\beta} - J_B r_A F_{2\gamma} + J_C r_A F_{2\beta}) r_B + ((J_A r_B F_{1\gamma} G_{2\gamma} - J_A r_B F_{2\gamma} G_{1\gamma} - J_B r_A F_{1\gamma} G_{2\gamma} + J_B r_A F_{2\gamma} G_{1\gamma} - J_C r_A r_B G_{2\gamma} + J_C r_A F_{1\beta} G_{2\gamma} + J_C r_A r_B F_{2\gamma} - J_C r_A F_{1\beta} F_{2\gamma} - J_C r_A F_{1\gamma} F_{2\beta}) T)} / ((J_A F_{1\beta} F_{2\gamma} - J_A F_{1\gamma} F_{2\beta} - J_B r_A F_{2\gamma} + J_C r_A F_{2\beta}) r_B) = 0 \tag{24}$$

$$\frac{(-J_A r_C F_{1\beta} + J_B r_A r_C - J_B r_A F_{1\gamma} + J_C r_A F_{1\beta}) g}{(J_A F_{1\beta} F_{2\gamma} - J_A F_{1\gamma} F_{2\beta} - J_B r_A F_{2\gamma} + J_C r_A F_{2\beta}) r_C - ((J_A r_C F_{1\beta} G_{2\gamma} - J_A r_C F_{2\beta} G_{1\gamma} - J_B r_A r_C G_{2\gamma} + J_B r_A F_{1\gamma} G_{2\gamma} - J_B r_A F_{2\gamma} G_{1\gamma} - J_C r_A F_{1\beta} G_{2\gamma} + J_C r_A r_C F_{2\beta} + J_C r_A F_{1\beta} F_{2\gamma} - J_C r_A F_{1\gamma} F_{2\beta}) T)} / ((J_A F_{1\beta} F_{2\gamma} - J_A F_{1\gamma} F_{2\beta} - J_B r_A F_{2\gamma} + J_C r_A F_{2\beta}) r_C) = 0 \tag{25}$$

In order to simplify or to use for other applications, we might require that each coefficient of g and T become zero in order to have analytic solution for the friction coefficients. Alternatively, one might examine the case $T = 0$. Otherwise, numerical solution will be required to solve the coupling system of Eqs. (24) - (25).

Note that the analysis is valid for hollow and full cylinders and in some 2D cases even for spheres. However, the only difference is expressed in the moment of inertia. We will assume that in order to have instability situation that expressed in mechanical detachment is fulfilled when one of the normal forces becomes zero by one of the following conditions:

$$N_{AB} = \frac{F_{k,AB}}{\mu_{BA}} = 0 \text{ and/or } N_{AC} = \frac{F_{k,AC}}{\mu_{CA}} = 0 \tag{26}$$

while $\mu_{BA}, \mu_{CA} \neq 0$. In other words, we might say (based on (19) – (20)) that:

$$\alpha_B = 0 \text{ and/or } \alpha_C = T/I_C \tag{27}$$

Substituting (27) into equations (27) – (28) lead to the similar relations as resulted in (24) – (25) that require the same numerical analysis as described above. Assuming that the denominators does not become zero.

Accordingly, one can deduce the angular velocity value, the friction coefficients and other cylinders geometrical parameters (cylinders diameter) in order to accommodate and ensure the system stability. In addition, in order to have better stability, exceptional the geometry importance, we might also recommend having better/improved contact by using flexible tighten belt.

4 Problem Formulation – Asymmetrical beam moment of stability margin by using broad/wide junction/connection

Suppose we have asymmetrical beam (or shaft) with asymmetrical mass distribution alongside different linear – saw section parts in the longitudinal direction leaning on broad joint connection as shown in Fig. 3.

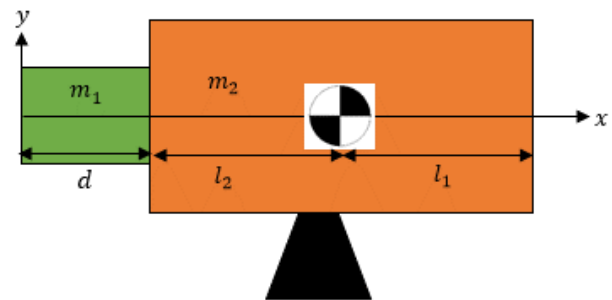


Figure 3: Asymmetrical beam illustration.

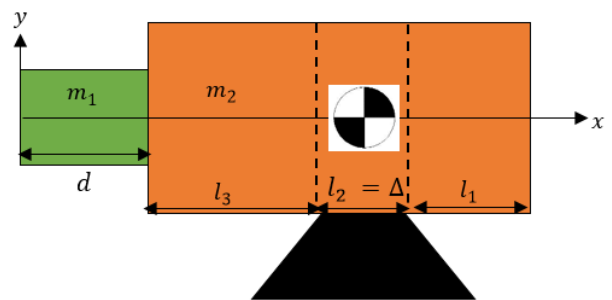


Figure 4: Sectioned asymmetrical beam illustration.

The system (the mass and the connector) is characterized by asymmetrical beam composed of two rigid connected mass - bodies m_1 and m_2 with appropriate length d and l , respectively. In addition, the total length of body-mass m_2 fulfills $l = l_1 + l_2$, whereas l_1 – represents the length from the right side of body-mass m_2 to the center of total mass and l_2 - represents the distance from the total center of mass to the left side of body-mass m_2 . The beam is laid on broad joint connection that might be flexible adjusted to the optimal width in relative to the total mass center of gravity. Those bodies could be cylindrical or rectangular

section shaft parts. Here, Cartesian coordinates system is being use alongside the longitudinal direction, while its origin is located. We also assume here for simplicity that y direction is symmetrical. Although the problem could be solved also with asymmetrical y direction considering that the center of gravity should be composed from x, y components.

It is well – known and can be easily proved by moment calculation that the center of gravity in case of joint – point is obtained by:

$$L_{C.G} = \frac{m_1(\frac{d}{2}+l)+m_2l}{m_1+m_2} \quad (28)$$

where $d/2$ represents the distance from the body-mass m_1 center to its right end. In more generalized way, equation (28) could be written by its components in x , y direction as:

$$L_{C.Gx} = \frac{m_1(\frac{d_x}{2}+l_x)+m_2l_x}{m_1+m_2} \quad (29)$$

$$L_{C.Gy} = \frac{m_1(\frac{d_y}{2}+l_y)+m_2l_y}{m_1+m_2} \quad (30)$$

Now, suppose that the current beam laid up on width joint connection instead of point connection joint. Therefore one would like to estimate the required width length (Δ) in order to keep on stabilized system.

In the first step, we will depart the domain into three sections as appear in Fig. 4.

The moment equilibrium along the x-axis will be describes as:

The moment equilibrium in the left side connection corner will be calculated by:

$$m_1g\left(\frac{d}{2} + l_3\right) + \frac{m_2g}{l}l_3\frac{l_3}{2} = \frac{m_2g}{l}l_1\left(\frac{l_1}{2} + \Delta\right) + \frac{m_2g}{l}\Delta\frac{\Delta}{2} \quad (31)$$

The moment equilibrium in the right side connection corner will be calculated by:

$$\frac{l_1^2}{2}\frac{m_2g}{l} = m_1g\left(\frac{d}{2} + l_3 + \Delta\right) + \frac{m_2g}{l}\Delta\frac{\Delta}{2} + \frac{m_2g}{l}l_3\left(\frac{l_3}{2} + \Delta\right) \quad (32)$$

whereas $l_3 = l - \Delta - l_1$.

Solving Eqs. (31) – (32) yields:

$$l_3 = \frac{1}{2} \frac{-dm_1 + lm_2}{m_1 + m_2} \quad (33)$$

$$\Delta = \frac{1}{2} \frac{1}{(m_1 + m_2)m_2} \left(dm_1m_2 - 2m_1^2l - 2m_1lm_2 - lm_2^2 + 2\sqrt{-dlm_1m_2 + l^2m_1^2 + m_2^2l_1^2}m_1 + 2\sqrt{-dlm_1m_2 + l^2m_1^2 + m_2^2l_1^2}m_2 \right) \quad (34)$$

4 Conclusion

In this study, we present a general framework for calculating displacement alongside stress-strain relationships of rotating FGM cylinder with exponential varying thickness and material properties subjected to mechanical and thermal loadings.

Also, body - force expressions dependent on geometry, gravity acceleration and friction coefficient to ensure stability of three cylinders rotating transmission system in triangle configuration with moment/torque friction were derived. The derived system can only be solved by numerical means.

Finally, asymmetrical beam (or shaft) with asymmetrical mass distribution alongside different linear – saw section parts in the longitudinal direction leaning on broad joint connection was examined by finding the total center of mass and determining the connection optimal width to ensure the asymmetrical beam stability.

In future, better mechanism approximations should be further study in the context of presented model in the following topics:

1. To develop improved and simplified stress-strain relations of cylindrical or conical bodies FGM material dependent of the displacement. This might be implemented by approximating Whittaker's functions using Wen-feng mentioned studies. Also, considering more phenomenon, like magnetic, electrical and to have more generalized solutions. Understanding the solutions range of validation and comparing them to real experiments.

2. Finding approximations for the above obtained expressions concerning the triangular transmission cylindrical system. Comparing them to real experiments. One might also use energy method for solution and comparison. Another extension might be applied using the study performed by Ott and Hyon [36] to generate oscillating balancing controlled system (robotic system).

3. Finding solutions for the above obtained expressions concerning the asymmetrical beam in case of three dimensional asymmetrical geometry.

References:

- [1] Durodola J. F., and Attia, O., "Deformation and stresses in functionally graded rotating disks". *Composites Science and Technology*, 60 987-995 (2000).
- [2] Damircheli, M., Azadi, M., Temperature and thickness effects on thermal and mechanical stresses of rotating FG-disks, *J. Mech. Sci. Tech.*, **25** (3) 827-836 (2011).
- [3] Asfar, A. M., and Go, J., Finite element analysis of thermoelastic field in a rotating FGM circular disk, *Applied Mathematical Modelling*, **34** 3309–3320 (2010)
- [4] Ali, A., Bayat, M., Sahari, B. B., Saleem, M., and Zaroog, O. S., The effect of ceramic in combinations of two sigmoid functionally graded rotating disks with variable thickness, *Scientific Research and Essays*, **7** (25), 2174-2188 (2012).
- [5] Thawait, A. K., Sondhi, L., Thermoelastic Analysis of Variable Thickness FGM Rotating Disk by Finite Element Method, *IJEMR*, 2394-6962 (2015).
- [6] Zheng, Y., Bahaloo, H. Mousanezhad, D., Mahdi, E., Vaziri A., and Nayeb-Hashemi, H., Stress analysis in functionally graded rotating disks with non-uniform thickness and variable angular velocity, *Int. J. Mech., Sci.*, 2016.
- [7] Zheng, Y., Bahaloo, H., Mousanezhad, D., Vaziri, A., and Nayeb-Hashemi, H. "Displacement and Stress Fields in a Functionally Graded Fiber-Reinforced Rotating Disk With Nonuniform Thickness and Variable Angular Velocity." *ASME. J. Eng. Mater. Technol.*, **139** (3) 031010 (2017).
- [8] Allam, M. N. M., Tantawy, R., and Zenkour, A. M., Thermoelastic stresses in functionally graded rotating annular disks with variable thickness, *J. Thero. App. Mech.*, **56**, 4, 1029-1041 Warsaw (2018).
- [9] Thawait, A. K., Sondhi, L., Sanyal, S., and Bhowmick, S., "Stress and Deformation Analysis of Clamped Functionally graded Rotating Disks with Variable Thickness" *Mechanics and Mechanical Engineering*, **23** (1) 202-211 (2019).
- [10] Baghani, M., Heydarzadeh, N., and Roozbahani, M. M., Stress analysis of a functionally graded micro/nanorotating disk with variable thickness based on the strain gradient theory, *International Journal of Applied Mechanics*, **8** (2) 1650020 (2016).
- [11] Behravan Rad, A., Shariyat, M., Three-dimensional magneto-elastic analysis of asymmetric variable thickness porous FGM circular plates with non-uniform tractions and Kerr elastic foundations, *Composite Structures*, **125** 558–574 (2015).
- [12] Shariyat, M., Mohammadjani, R., Three-dimensional compatible finite element stress analysis of spinning two-directional FGM annular plates and disks with load and elastic foundation non-uniformities, *Lat. Am. j. solids struct.* **10** (5) 859-890 (2013).
- [13] Shariyat, M., Mohammadjani, R., Three-dimensional stress field analysis of rotating thick bidirectional functionally graded axisymmetric annular plates with nonuniform loads and elastic foundations. *Journal of Composite Materials*, **48** (23) 2879-2904 (2014).
- [14] Sarkar P. R., Rahman A. S., Effect of magnetic field on the thermo-elastic response of a rotating FGM Circular disk with non-uniform thickness, *The Journal of Strain Analysis for Engineering Design*, **57** (2) 116-131 (2021).

- [15] Eraslan, A. N., and Orcan, Y., Elastic-plastic deformation of a rotating solid disk of exponentially varying thickness, *Mechanics of Materials* **34** 423–432 (2002).
- [16] Zenkour, A. M., Analytical solutions for rotating exponentially – graded annular disks with various boundary conditions, *International Journal of Structural Stability and Dynamics*, **5** (4) 557-577 (2005).
- [17] Zenkour, A. M., Steady-state thermoelastic analysis of a functionally graded rotating annular disk, *International Journal of Structural Stability and Dynamics*, **6** (4) 559-573 (2006).
- [18] Zenkour, A. M., Elastic deformation of the rotating functionally graded annular disk with rigid casing, *J. Mater. Sci.*, **42** 9717-9724 (2007).
- [19] Zenkour, A. M., Stress distribution in rotating composite structures of functionally graded solid disks, *J. Mat. Process. Tech.*, **209** 3511-3517 (2009).
- [20] Chen, J., Ding, H., and Chen, W., "Three-dimensional analytical solution for a rotating disc of functionally graded materials with transverse isotropy", *Arch. Appl. Mech.*, **77**, 241–251 (2007).
- [21] Sharma, J. N., Sharma, D., and Kumar, S., Stress and strain analysis of rotating FGM thermoelastic circular disk by using FEM, *IJPAM*, **74** (3) 339 – 352 (2012).
- [22] Jabbari, M., Ghannad, M., and Nejad, M. Z., Effect of thickness profile and FG function on rotating disks under thermal and mechanical loading, *Journal of Mechanics*, **32** (1), 35-46 (2016).
- [23] Manthenaa, V. R., Lambab, N. K., and Kedara, G. D., Thermal stress analysis in a functionally graded hollow elliptic-cylinder subjected to uniform temperature distribution, *Appl. Appl. Math.*, **12** (1) 613-632 (2017).
- [24] Dai, T., and Dai, H. L., Thermo-elastic analysis of a functionally graded rotating hollow circular disk with variable thickness and angular speed, *Applied Mathematical Modelling*, **40** 7689–7707 (2016).
- [25] Akbari, M. R., and Ghanbari, J., Analytical exact solution for functionally graded rotating disks under non-symmetric thermal and mechanical loads, *Mater. Res. Express*, **6** 056545 (2019).
- [26] Lin, W. F., "Analytic deformation and stresses solutions of functionally graded rotating disk under mechanical and thermal load", *2019 4th International Conference on Automation, Mechanical and Electrical Engineering (AMEE 2019)*, 265-271 (2019).
- [27] Lin, W. F., "Elastic analysis for rotating functionally graded annular disk with exponentially-varying profile and properties", *Mathematical Problems in Engineering*, Article ID 2165804 (2020).
- [28] Lin, W. F., "Analysis of Thick-Wall Hollow Functionally Graded Material under Temperature and Pressure Loads", *IEEE Eurasia Conference on IOT, Communication and Engineering (ECICE)*, 279-281 (2020).
- [29] Lin, W. F., "Stress analysis of thick-Wall hollow functionally graded material based on plane strain problem", *J. Phys.: Conf. Ser. (MSEE 2020)*, **1838** 012006 (2020).
- [30] Paul, S. K., and Shani, M., "Stress analysis of functionally graded disk with exponentially varying thickness using iterative method", *WSEAS TRANS. on APP. and THEOR. MECH.*, **16** 232-244 (2021)
- [31] Hibbeler, R.C. Engineering Mechanics: Statics & Dynamics (11 Ed.). Pearson, Prentice Hall. 441–442, (2007).
- [32] Alrasheed, S., Principles of mechanics: fundamentals university physics, *IEREK - springer*, 124-132 (2019).
- [33] Zéhil, G.P., Gavin, H.P. (2013). "Simplified approaches to viscoelastic rolling resistance", *IJSS* **50** (6): 853–862 (2013).
- [34] Koczan, G. M., Ziomek, J., Research on rolling friction's dependence on ball bearings' radius, *Przegląd Mechaniczny* 1-9 (2019).
- [35] Ndiaye, B.C., Gao, Z., Fall, M., Zhang, Y., "Effect of the Rolling Friction on the Heap Formation of Dry and Wet Coarse Discs". *Appl. Sci.* 2021, **11**, 6043.
- [36] Ott C., Hyon, S. H., Torque-Based Balancing. In: Goswami A., Vadakkepat P. (eds) *Humanoid Robotics: A Reference*. Springer, Dordrecht. 79-101, (2017)
- [37] Das, A., Alagirusamy, R., "3 - Fundamental principles of open end yarn spinning", *In Woodhead Publishing Series in Textiles, Advances in Yarn Spinning Technology*, Woodhead Publishing (2010).

Conflict of interest statement

On behalf of all authors, the corresponding author states that there is no conflict of interest

Contribution of individual authors to the creation of a scientific article (ghostwriting policy)

The author' own fully creation.

Follow: www.wseas.org/multimedia/contributor-role-instruction.pdf

Sources of funding for research presented in a scientific article or scientific article itself

No scientific funding is involved.